Title
Rejuvenation of extensively passaged human chondrocytes to engineer functional articular cartilage.

Journal
Biofabrication, 13(3)

ISSN
1758-5082

Authors
Kwon, Heenam
Brown, Wendy E
O'Leary, Siobhan A
et al.

Publication Date
2021-07-01

DOI
10.1088/1758-5090/abd9d9

Peer reviewed

Biofabrication

PAPER

Rejuvenation of extensively passaged human chondrocytes to engineer functional articular cartilage

Heenam Kwon[1], Wendy E Brown[1], Siobhan A O'Leary[2], Jerry C Hu[1] and Kyriacos A Athanasiou[1]

[1] Department of Biomedical Engineering, University of California, Irvine, Irvine, CA, United States of America
[2] Align Technology Inc., San Jose, CA, United States of America

E-mail: athens@uci.edu

RECEIVED
2 October 2020

REVISED
14 December 2020

ACCEPTED FOR PUBLICATION
8 January 2021

PUBLISHED
2 April 2021

Keywords: human articular chondrocytes, cell expansion, highly passaged chondrocytes, aggregate rejuvenation, phenotype restoration, scaffold-free tissue engineering

Supplementary material for this article is available online

Abstract

Human articular chondrocytes (hACs) are scarce and lose their chondrogenic potential during monolayer passaging, impeding their therapeutic use. This study investigated (a) the translatability of conservative chondrogenic passaging and aggregate rejuvenation on restoring chondrogenic properties of hACs passaged up to P9; and (b) the efficacy of a combined treatment of transforming growth factor-beta 1 (TGF-β1) (T), chondroitinase-ABC (C), and lysyl oxidase-like 2 (L), collectively termed TCL, on engineering functional human neocartilage via the self-assembling process, as a function of passage number up to P11. Here, we show that aggregate rejuvenation enhanced glycosaminoglycan (GAG) content and type II collagen staining at all passages and yielded human neocartilage with chondrogenic phenotype present up to P7. Addition of TCL extended the chondrogenic phenotype to P11 and significantly enhanced GAG content and type II collagen staining at all passages. Human neocartilage derived from high passages, treated with TCL, displayed mechanical properties that were on par with or greater than those derived from low passages. Conservative chondrogenic passaging and aggregate rejuvenation may be a viable new strategy (a) to address the perennial problem of chondrocyte scarcity and (b) to successfully rejuvenate the chondrogenic phenotype of extensively passaged cells (up to P11). Furthermore, tissue engineering human neocartilage via self-assembly in conjunction with TCL treatment advances the clinical use of extensively passaged human chondrocytes for cartilage repair.

1. Introduction

Human articular chondrocytes (hACs) are used clinically to repair cartilage lesions. In addition to current surgical approaches including microfracture, mosaicplasty, and cell-based techniques (e.g., matrix-induced autologous chondrocyte implantation [1–3], a variety of tissue-engineered cartilage products derived from expanded hACs are in the developmental pipeline [4, 5]. Limited cellularity in cartilage requires passaging to obtain sufficient cells, but chondrocytes are prone to dedifferentiation during expansion [6]. Strategies to retain chondrogenic potential of hACs while expanding are necessary to advance cell-based therapies for cartilage.

Monolayer chondrocyte expansion results in rapid dedifferentiation [6, 7], characterized by type I collagen expression [7] and fibroblastic morphology [8]. Articular chondrocytes at up to passage 3 (P3) have been reported as used in tissue engineered cartilage products for clinical trials in the pipeline [4, 5]. Extensively passaged cells (i.e. $\geqslant$P3) barely or no longer generate cartilage-specific matrix proteins (e.g. aggrecan and type II collagen) [9], which diminish in a passage number-dependent manner [6]. While P1 chondrocytes formed tissues containing glycosaminoglycan (GAG) and type II collagen, P5 cells no longer exhibited chondrocytic morphology or produced cartilage-specific matrix [10]. To overcome such limits, various media and

3D culture systems have been examined to retain or to improve the chondrogenic potential of passaged chondrocytes [11–14]. Despite these endeavors, it is still recognized that phenotypic changes in passaged chondrocytes hamper their clinical use, particularly when cells at P3 or higher are required due to cell scarcity.

Culturing cells in 3D aggregates prior to neocartilage formation appears to be beneficial to chondrocyte redifferentiation [15]. Previously, the effect of aggregate culture on the chondrogenic properties of hACs has been demonstrated [16]. In this prior study, with aggregate culture, hACs expressed significantly increased chondrogenic gene expression (i.e. Col2A1, Col2A1/Col1A1 ratio, Sox9, and ACAN expression) when compared to cells that did not undergo aggregate culture, suggesting that aggregate culture has an ability to improve chondrogenic properties of hACs. Furthermore, the effect of exogenous growth factors during aggregate culture has also been demonstrated. In particular, 'aggregate redifferentiation', an aggregate culture in the presence of TGF-β1, enhances the post-expansion chondrogenic phenotype of chondrocytes, allowing their use in tissue engineering [16, 17]. Aggregate redifferentiation has been used on P7 leporine chondrocytes, allowing them to yield functional neocartilage [18]. Another version of aggregate redifferentiation, combining aggregate culture with a growth factor cocktail of transforming growth factor-beta 1 (TGF-β1), bone morphogenetic protein-2 (BMP-2), and growth differentiation factor-5 (GDF-5), promoted P2 hACs to express chondrogenic genes, such as Sox9, ACAN, and Col2A1, and further enhanced cartilage matrix production [17]. However, despite significant results regarding this process (termed 'aggregate rejuvenation'), questions remain on whether the efficacy can be replicated for extensively passaged human chondrocytes.

Toward applying tissue-engineered neocartilage in joint repair, generating neocartilage that is not only engineered from appropriate redifferentiated chondrocytes but also exhibits suitable functional properties to sustain mechanical load *in vivo* is critical. Engineering neocartilage constructs with TGF-β1, chondroitinase-ABC (c-ABC), and lysyl oxidase-like 2 (LOXL2), has been shown to improve neocartilage functional properties (i.e. biochemical and mechanical properties). TGF-β1 is well-known for inducing chondrogenesis [19] and increasing neocartilage functional properties [20, 21]. C-ABC, an enzyme that degrades GAG, enhances neocartilage collagen content and tensile properties [22–24]. LOXL2 creates pyridinoline (PYR) crosslinks between collagen fibers [25, 26], yielding improvements in neocartilage tensile properties [27]. In response to TGF-β1 and c-ABC, engineered bovine neocartilage exhibited enhanced functional properties when compared to individual factors [28]. A combined treatment of TGF-β1, c-ABC, and LOXL2 (termed TCL) was more effective in enhancing functional properties of engineered bovine neofibrocartilage when compared to other combinations [29]. Importantly, the efficacy of TCL treatment at neocartilage formation was successfully translated to human neocartilage derived from P3 hACs [30]. However, it is unknown whether these stimuli can continue to be applicable to human neocartilage derived from extensively passaged chondrocytes to enhance functional properties.

Inasmuch as extensively passaged hACs have not been successfully used to engineer human neocartilage, the study's objectives were: (a) to translate conservative chondrogenic passaging and aggregate rejuvenation on extensively passaged hACs to yield chondrocytes suitable for engineering human neocartilage of sufficient functionality; and (b) to augment the effects of conservative chondrogenic passaging and aggregate rejuvenation on extensively passaged hACs by employing TCL treatment to fabricate functional human neocartilage. The scaffold-free, self-assembling process [31, 32], previously demonstrated to generate mechanically robust neocartilage, was used to form human neocartilage. It was hypothesized that the efficacy of aggregate rejuvenation in improving chondrogenic properties would be applicable to human cells at high passages (i.e. P7 and P9). It was also hypothesized that aggregate rejuvenation, followed by TCL treatment, would revert hACs at high passages (e.g., P7, P9, and P11) to a chondrogenic phenotype and lead to the formation of mechanically robust human neocartilage on par with those formed by hACs at lower passages (e.g., P3 and P5).

2. Methods

2.1. Human articular chondrocyte isolation and expansion

Chondrocytes were isolated from human articular cartilage from the knees of three donors without signs of musculoskeletal pathology. The donor tissues were obtained from the Musculoskeletal Transplant Foundation (Kansas City, MO) under an IRB exemption as it does not constitute as human subject research; the donor tissues were discarded samples from deidentified donors. These donors were a 43 year-old Caucasian male (donor 1), a 18 year-old Hispanic female (donor 2), and a 34 year-old Caucasian male (donor 3). Cells from different donors were not intermixed. Donors 2 and 3 were used to examine the study's repeatability. Minced cartilage was digested in 0.2% collagenase type II (Worthington, Lakewood, NJ) solution containing 3% fetal bovine serum (FBS, Atlanta Biologicals, Lawrenceville, GA) for 18 h at 37 °C, followed by filtration through a 70 μm strainer. Isolated cells were counted, resuspended in freezing medium

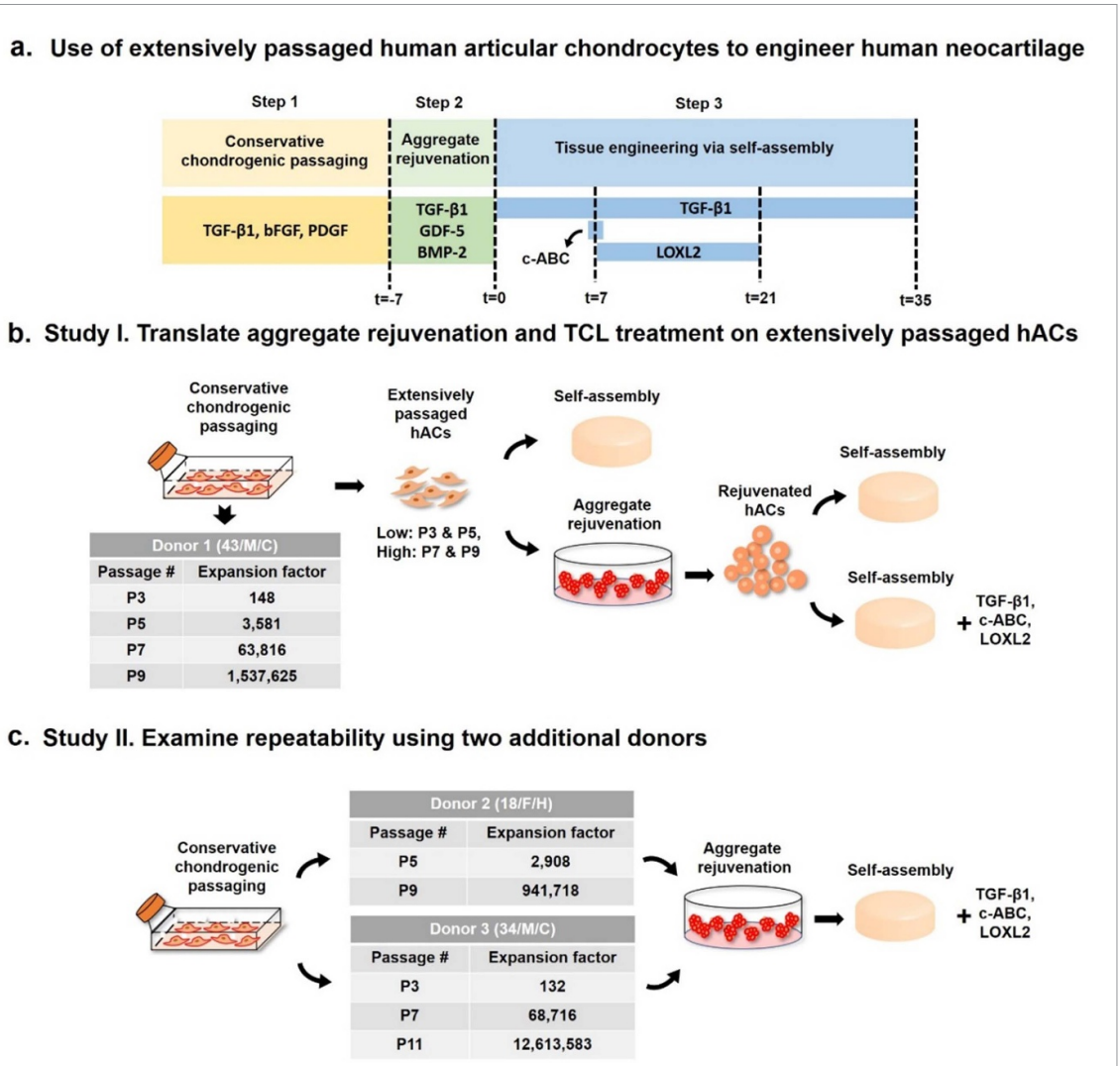

Figure 1. Schematic diagram of the study. (a) Use of extensively passaged hACs to engineer human neocartilage. Three steps are involved: (1) conservative chondrogenic passaging, (2) aggregate rejuvenation, and (2) tissue engineering via self-assembly. (b) Study I: the effects of aggregate rejuvenation and TCL treatment on engineering functional human neocartilages derived from extensively passaged hACs (up to P9 with an expansion factor of ∼1.5 million) from donor 1 were evaluated. (c) Study II: repeatability of the treatments was examined using two additional donors (donors 2 and 3). Donor 2's hACs were expanded up to P9 with an expansion factor of ∼94 000, and donor 3's hACs were expanded up to P11 with an expansion factor of ∼12.6 million.

consisting of 90% FBS and 10% dimethyl sulfoxide, and stored in liquid nitrogen until use. For expansion, a conservative chondrogenic passaging method was used, based on a previously reported chondrogenically tuned expansion [33] (figure 1). Briefly, hACs were seeded at 25 000 cells cm^{-2} and expanded in chondrogenic culture medium (CHG) (DMEM with high glucose/GlutaMAX™, 1% penicillin–streptomycin–fungizone (P/S/F), 1% non-essential amino acids (Gibco), 1% ITS+ premix (BD Biosciences), 50 μg ml^{-1} ascorbate-2-phosphate, 40 μg ml^{-1} L-proline, 100 μg ml^{-1} sodium pyruvate, and 100 nM dexamethasone), supplemented with 2% FBS, 1 ng ml^{-1} TGF-β1 (Peprotech, Rocky Hills, NJ), 5 ng ml^{-1} bFGF (Peprotech), and 10 ng ml^{-1} PDGF (Peprotech). Cells were passaged using 0.05% trypsin-EDTA (Gibco), followed by 0.2% collagenase type II solution containing 3% FBS, and frozen at P2, P4, P6, P8, and/or P10 in liquid nitrogen until use. After thawing, cells underwent one more passage, leading to P3, P5, P7, P9 and/or P11; cells then underwent either (a) self-assembly (control) or (b) aggregate rejuvenation followed by self-assembly. Cell expansion metrics were calculated [18] using cell doubling number = log(expansion factor)/log(2); expansion factor = final cell number/initial cell number (supplemental table 1 (available online at stacks.iop.org/BF/13/035002/mmedia)).

2.2. Chondrogenic differentiation in aggregate rejuvenation

Cells at P3, P5, P7, and P9 derived from donor 1 were seeded at 750 000 cells ml^{-1} in 1% agarose-coated plates for aggregate rejuvenation. The plates were placed on an orbital shaker for 24 h to allow for cells to form aggregates, and the aggregates were maintained in CHG supplemented with 10 ng ml^{-1}

TGF-β1, 100 ng ml^{-1} GDF-5, and 100 ng ml^{-1} BMP-2 for 7 d [16, 17]. Then, aggregates were digested using 0.05% trypsin-EDTA for 45 min, followed by 0.2% collagenase type II solution containing 3% FBS for up to 2 h. For the repeatability study, cells at P5 and P9 derived from donor 2 and cells at P3, P7, and P11 derived from donor 3 underwent aggregate rejuvenation. The resulting cells were self-assembled to form neocartilage (figure 1).

2.3. Neocartilage self-assembly

Neocartilage was formed using the self-assembling process as previously described [31, 32]. Briefly, 2% agarose wells were formed in 48 well plates using custom-made stainless-steel molds with 5 mm diameter cylindrical prongs. The wells were washed with DMEM with high glucose/GlutaMAX™ containing 1% P/S/F twice prior to seeding. Suspended in 100 μl of CHG supplemented with 200 units ml^{-1} hyaluronidase type I-S from bovine testes (Sigma Aldrich, St. Louis, MO) and 2 μM cytochalasin D (Enzo life Sciences, Farmingdale NY), 2 $\times$ 10^6 hACs were seeded in each well. After seeding for 4 h, an additional 400 μl of CHG supplemented with 2 μM cytochalasin D was added to the wells. Medium was exchanged every 24 h, and cells were treated with 2 μM cytochalasin D for the first 72 h. After neocartilage constructs were unconfined from the wells, medium was exchanged every other day. The self-assembled human neocartilages were maintained for 5 weeks.

2.4. TCL treatment

Control constructs were maintained in CHG. For the TCL-treated group, constructs were maintained in CHG supplemented with 10 ng ml^{-1} TGF-β1. On $t = 7$ d, constructs were treated once with 2 unit ml^{-1} of c-ABC (Sigma Aldrich) for 4 h at 37 °C, followed by a 10 min, 1 mM zinc sulfate quench at 37 °C. From t = 7–21 d, 0.15 μg ml^{-1} of LOXL2 (SignalChem, Richmond, BC, Canada), 0.146 mg ml^{-1} hydroxylysine, and 1.6 μg ml^{-1} copper sulfate were added (figure 1).

2.5. Mechanical testing and biochemical evaluation

After 5 weeks, samples were mechanically tested. For compressive testing, samples were preconditioned with 15 cycles at 5% compressive strain using an Instron 5565. At a strain rate of 1% sample height per second, incremental stress-relaxation was performed for 10% and 20% strain. Relaxation modulus (E_r), instantaneous modulus (E_i), and coefficient of viscosity (η) were calculated using a standard linear solid model [34]. For tensile testing, samples were created in the shape of dog bones using dermal punches; in general, sample dimensions were 4.7 $\pm$ 0.8 mm (length) by 0.5 $\pm$ 0.1 mm (width). The samples were photographed, and the ends of the dog bones were glued to paper tabs with the narrow region of the dog bone exposed within a gauge length of 1.3 mm. The cross-sectional area of the samples was measured by Image J. The samples on the paper were placed into grippers. A TestResources 840L or an Instron 5565 was used to track force and displacement over time as the samples deformed under uniaxial testing. Samples were pulled apart at a constant rate of 1% of the gauge length per second until failure, and a force-displacement curve was generated. Using the cross-sectional area and the gauge length, data were converted to a stress–strain curve, from which the Young's modulus (E_Y), ultimate tensile strength (UTS), toughness (U_T), resilience (U_r), and strain at failure values were derived.

For biochemical assays, wet weights (WWs) of samples were recorded. Lyophilized samples were digested in 125 μg ml^{-1} papain (Sigma Aldrich) in 50 mM phosphate buffer containing 2 mM N-acetyl cysteine (Sigma Aldrich) and 2 mM EDTA for 18 h at 60 °C. GAG was quantified using the Blyscan GAG Assay kit (Biocolor, Newtownabbey, Northern Ireland). Total collagen content was assessed using a modified chloramine-T hydroxyproline assay [35] and a SIRCOL collagen standard (Accurate Chemical and Scientific Corp, Westbury, NY).

2.6. Histology and immunohistochemistry

Formalin-fixed samples were paraffin-embedded, sectioned, and stained with hematoxylin and eosin (H&E); safranin-O and fast green. Immunohistochemical staining for collagen I and II used rabbit anti-type I collagen (Abcam, Cambridge, MA) and rabbit anti-type II collagen (Abcam), using Vectastain ABC and DAB substrate kits (Vector Laboratories, Inc, Burlingame, CA).

2.7. Statistics

All data are shown in mean $\pm$ SD. Statistical differences among conditions were analyzed using one-way ANOVA with Tukey's *post hoc* test ($p < 0.05$) (JMP12). Statistically significant differences are shown by bars not sharing the same letter.

3. Results

3.1. Gross morphological and histological evaluation of human neocartilage

3.1.1. Study I: generation of human neocartilage (donor 1)

For donor 1, untreated P3 and P5 neocartilage constructs were curled and folded. Untreated P7 and P9 hACs formed spherical constructs (figure 2). Treated with aggregate rejuvenation, P3 and P5 hACs self-assembled into flat constructs, and P7 hACs generated flat constructs with significantly smaller diameter (4.4 $\pm$ 0.2 mm) than treated P3 and P5 constructs (6.1 $\pm$ 0.2 mm and 6.4 $\pm$ 0.1 mm, respectively; $p < 0.05$). With aggregate rejuvenation,

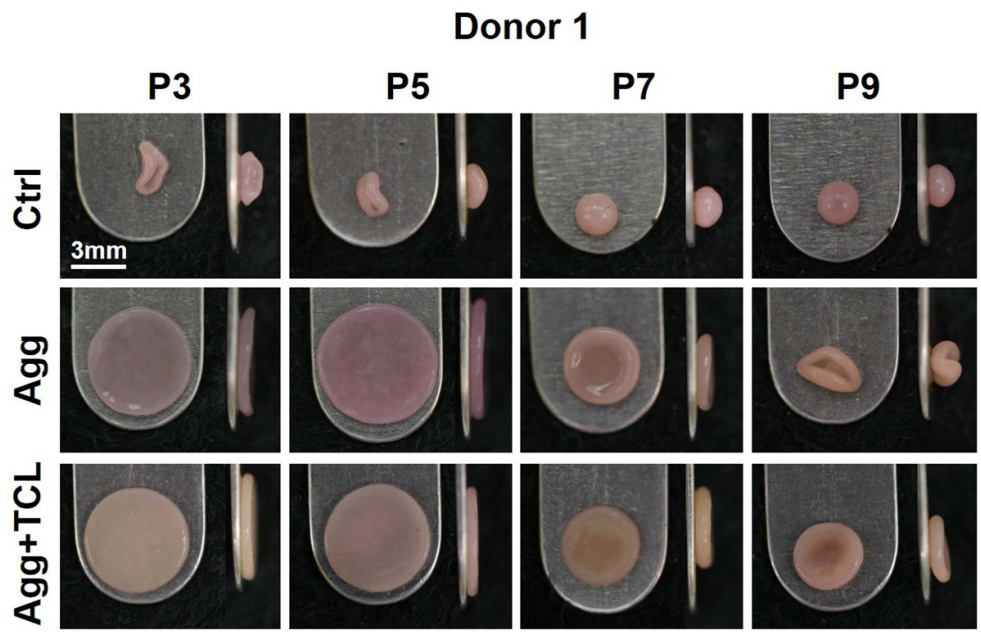

Figure 2. Gross morphology of human neocartilage derived from donor 1. Top and side views of human neocartilage constructs derived from P3, P5, P7, and P9. The effects of no treatment (Ctrl), aggregate rejuvenation (Agg), and aggregate rejuvenation followed by TCL treatment (Agg + TCL) on human neocartilage derived from P3, P5, P7, and P9 are shown. Abbreviations: TCL, TGF-β1 + c-ABC + LOXL2.

P9 constructs were curled and folded, similar to P3 and P5 untreated controls (figure 2).

TCL treatment following aggregate rejuvenation yielded more opaque morphologies at P3 and P5, when compared to aggregate rejuvenation treatment only. TCL treatment allowed P7 and P9 hACs to form flat constructs but with significantly smaller diameters (4.3 $\pm$ 0.0 mm and 3.8 $\pm$ 0.1 mm, respectively) when compared to P3 and P5 constructs (5.7 $\pm$ 0.1 mm, 5.7 $\pm$ 0.1 mm, respectively; $p < 0.05$) (figure 2).

Histologically, untreated human neocartilage did not display the spherical cell morphology associated with chondrocytes (figure 3(a)) at any of the examined passage numbers. With aggregate rejuvenation, P3 and P5 hACs were spherical and embedded in lacunae. However, as the passage number increased, presence of lacunae gradually diminished; treated P9 control constructs barely exhibited lacunae and, instead, contained fibroblast-like cells. TCL treatment following aggregate rejuvenation resulted in the presence of spherical cells residing in lacunae for all passages examined (figure 3(a)).

With aggregate rejuvenation, human neocartilage at all passage numbers stained for safranin-O and showed significantly more intense staining compared to control neocartilage (figure 3(b)). However, staining intensity decreased with increasing passage number. TCL treatment following aggregate rejuvenation further enhanced safranin-O intensity. Staining intensities were comparable at P3 and P5, and, to some extent, the intensity decreased in P7 and P9 constructs.

Aggregate rejuvenation by itself increased type II collagen staining over controls at all passages, though staining intensity decreased with increasing passage number (figure 3(c)). TCL treatment led to greater type II collagen staining (figure 3(a)) at all passages compared to aggregate rejuvenation treatment only. Interestingly, with aggregate rejuvenation, more intense type I collagen was observed in P5 and P7 constructs compared to P3 and P9 constructs (figure 3(d)). TCL-treated P3 and P5 constructs were negative for type I collagen staining, though at P7 and P9 treatment yielded constructs with minimal staining.

3.1.2. Study II: repeatability (donors 2 and 3)

Aggregate rejuvenation and TCL treatment were applied to form neocartilage derived from two additional donors. Untreated P5 control constructs derived from donor 2 were curled and folded, similar to untreated P3 and P5 control constructs from donor 1. Untreated P9 control constructs formed thin and relatively flat constructs with small diameter (<3 mm). In contrast, with aggregate rejuvenation and TCL treatment, P5 and P9 hACs yielded opaque and flat constructs. Similar gross morphologies were observed in neocartilages from donor 3. Untreated control constructs at all passages (P3, P7, and P11) exhibited either curled, folded, or spherical shapes. With treatment, cells at all passages formed neocartilages with flat morphologies. Consistent with the gross morphology of neocartilage from donor 1, treated donors 2 and 3 neocartilages at high passages displayed significantly smaller diameters (donor 2 P9:

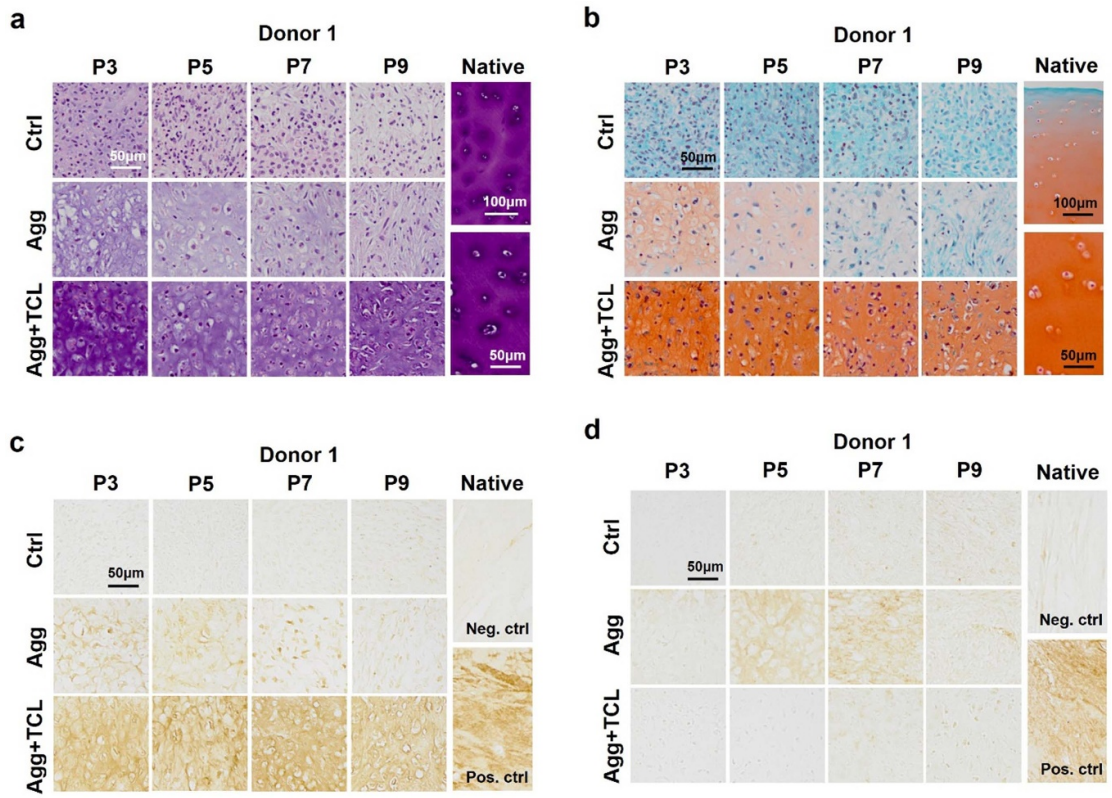

Figure 3. Histology and immunohistochemistry of human neocartilage derived from donor 1. (a) H&E, (b) safranin-O staining, (c) type II collagen staining, and (d) type I collagen staining of human neocartilage constructs derived from P3, P5, P7, and P9. The effects of no treatment (Ctrl), aggregate rejuvenation (Agg), and aggregate rejuvenation followed by TCL treatment (Agg + TCL) on human neocartilage are shown. Nucleus pulposus from human native intervertebral disc was used for positive and negative controls for type II and I collagen, respectively. Annulus fibrosus was used for positive and negative controls for type I and II collagen, respectively.

4.7 ± 0.1 mm, donor 3 P7 and P9: 4.1 ± 0.0 mm and 4.3 ± 0.1 mm, respectively) when compared to those derived from cells at low passages (donor 2 P5: 5.4 ± 0.1 mm, donor 3 P3: 5.2 ± 0.1 mm; $p < 0.05$) (figure 4(a)).

Untreated control neocartilages from donors 2 and 3 at any passage number did not contain cells with spherical morphology. With treatment, neocartilages from both donors exhibited chondrocytes embedded in lacunae at all passage numbers (figure 4(b)). Treated neocartilages showed significantly enhanced staining of safranin-O and type II collagen, and exhibited significantly decreased staining of type I collagen at all passage numbers, when compared to untreated control neocartilages (figure 5).

3.2. Biochemical and mechanical properties of human neocartilage

3.2.1. Study I: generation of human neocartilage (donor 1)

Aggregate rejuvenation, with or without TCL treatment, exhibited a range of enhancements in donor 1 neocartilage's biochemical and mechanical properties at different passages (figure 6). GAG per WW (GAG/WW) tended to decrease with increasing passage number (figure 6(a)) in untreated control neocartilages. With aggregate rejuvenation only, GAG/WW at every passage was significantly higher (3 to 4-fold) compared to controls. At each passage, when TCL was appliedGAG/WW further increased from aggregate rejuvenation treatment only by 1–4.5-fold. With TCL treatment, GAG content for P7 and P9 constructs was on par with that of P3 and P5 constructs. Total collagen content per WW (COL/WW) was highest in P5 control constructs compared to control constructs at other passages (figure 6(b)). Although COL/WW in P3 and P5 constructs was significantly decreased with aggregate rejuvenation by 50% and 65%, respectively, P7 and P9 constructs showed increased COL/WW by 57% and 157%, respectively, over control neocartilages. COL/WW was further increased in human neocartilage at each passage with TCL treatment by 0.3–1.8-fold when compared to human neocartilage with aggregate rejuvenation treatment only.

Control constructs were not testable for compression and tension at any passage (figure 6). With aggregate rejuvenation, P3, P5, and P7 constructs demonstrated compressive relaxation modulus and instantaneous modulus values that were not statistically different, while P9 constructs were not evaluated in compression due to their shape

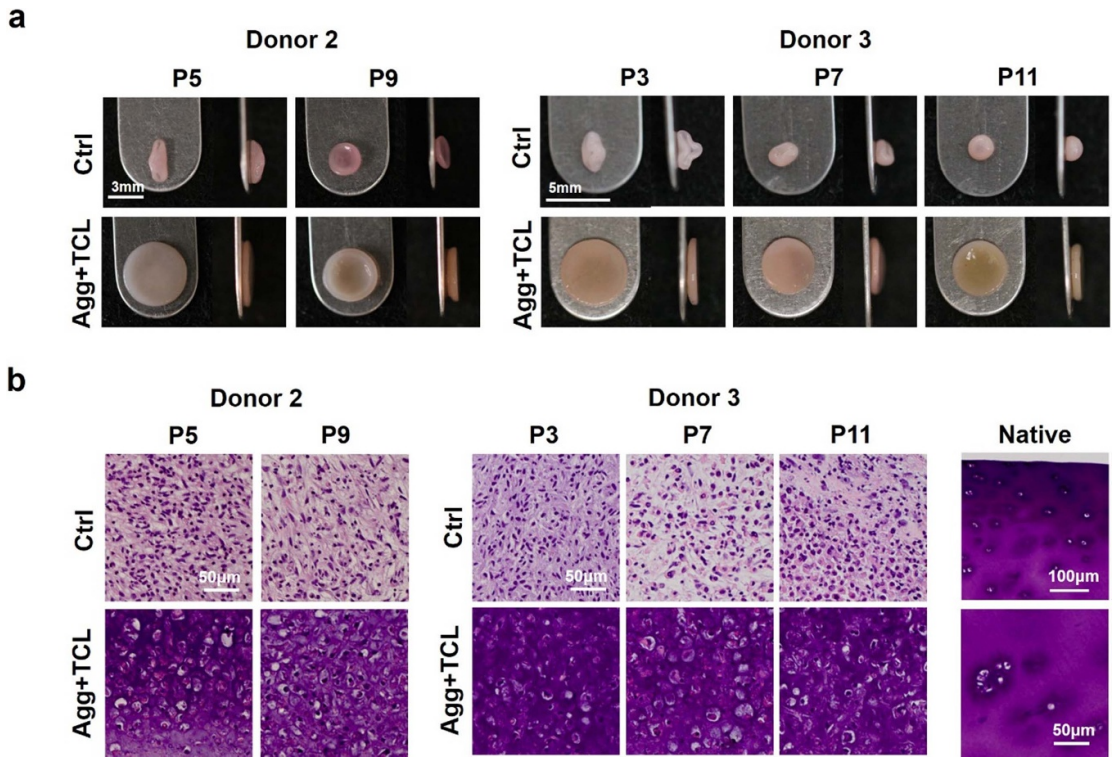

Figure 4. Gross morphology and H&E staining of human neocartilage derived from donors 2 and 3. (a) Top and side views and (b) H&E staining of neocartilage constructs derived from P5 and P9 donor 2 hACs, and from P3, P7, and P11 donor 3 hACs. The effects of no treatment (Ctrl), and aggregate rejuvenation followed by TCL treatment (Agg + TCL) on human neocartilage are shown.

(figures 6(c) and (d)). The relaxation modulus value of P7 constructs treated with TCL was 1.4-fold of P7 constructs treated with aggregate rejuvenation treatment only. Compressive instantaneous modulus was significantly increased with TCL treatment in neocartilage at P3, P5, and P7, by 1.6–2.7-fold when compared to neocartilage with only aggregate rejuvenation. The compressive properties were not statistically different, regardless of passage number, among the TCL-treated constructs. No significant difference in coefficient of viscosity was observed regardless of treatment and passage number (supplemental figure 1). With aggregate rejuvenation, tensile stiffness and strength exhibited comparable values among P3, P5, and P7 constructs, whereas P9 constructs demonstrated significantly enhanced tensile properties when compared to constructs from other passages (figures 6(e) and (f)). Toughness and resilience of P9 constructs were significantly higher than those of P3, P5, and P7 constructs, an effect which was also seen with tensile stiffness and strength (supplemental figure 1). Addition of TCL treatment significantly increased tensile stiffness in human neocartilage at P3, P5, and P7 by 20.0-fold, 12.5-fold, and 4.8-fold, respectively, and tensile strength by 5.0-fold, 3.5-fold, and 1.3-fold, respectively, when compared to aggregate rejuvenation treatment only. Tensile properties in TCL-treated P9 constructs were comparable to the properties in P9 constructs with aggregate rejuvenation treatment only. No significant difference in tensile properties was observed among TCL-treated human neocartilage. TCL-treated constructs showed comparable toughness, resilience, and strain at failure regardless of passage number (supplemental figure 1)

3.2.2. Study II: repeatability (donors 2 and 3)

Aggregate rejuvenation and TCL treatment allowed neocartilages for both donors 2 and 3 at high passage numbers to exhibit improved biochemical properties compared to their respective untreated control neocartilages (figure 7(a)). Aggregate rejuvenation and TCL treatment allowed P5 and P9 cells from donor 2 to form constructs with significantly higher GAG/WW and COL/WW by 14.0 to 21.5-fold and 1.4 to 2.0-fold, respectively, when compared to no treatment. With treatment, P9 constructs produced significantly decreased GAG/WW compared to P5 constructs. With regard to donor 3, treated constructs at all passage numbers produced significantly higher amount of GAG when compared to untreated controls by 22.0 to 29.0-fold. Interestingly, COL/WW was significantly higher in treated P7 and P11 constructs compared to treated P3 constructs by 0.9 and 1.3-fold, respectively and their respective untreated control constructs by 0.1 to 2.0-fold.

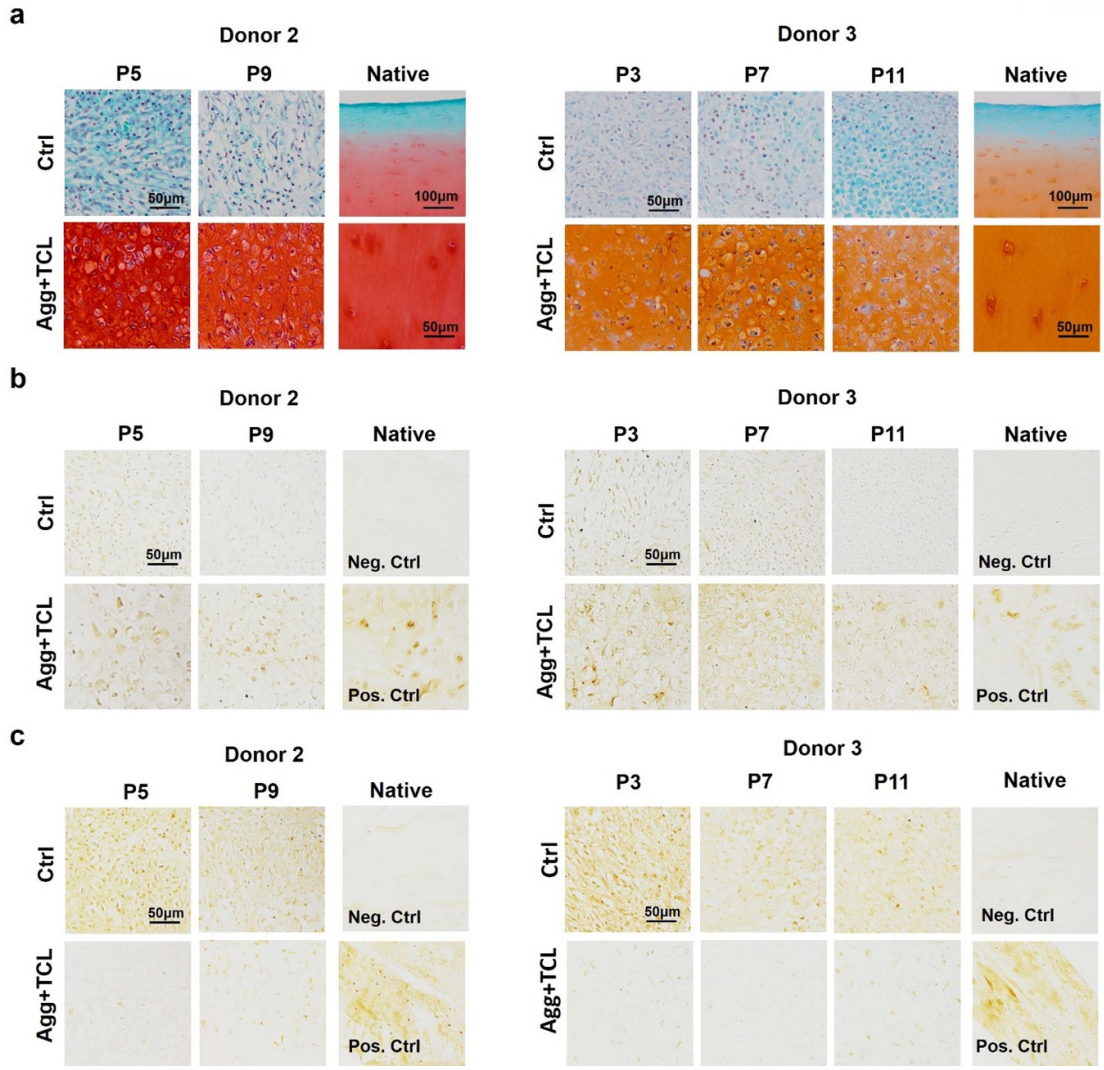

Figure 5. Safranin-O staining and immunohistochemistry of human neocartilage derived from donors 2 and 3. (a) Safranin-O staining, (b) type II collagen, and (c) type I collagen of neocartilage constructs derived from P5 and P9 donor 2 hACs, and from P3, P7, and P11 donor 3 hACs. The effects of no treatment (Ctrl), and aggregate rejuvenation followed by TCL treatment (Agg + TCL) on human neocartilage are shown.

As with donor 1, aggregate rejuvenation and TCL treatment significantly increased the mechanical properties of neocartilages, compared to control neocartilages from donors 2 and 3 (figures 7(b) and (c)). Treated P9 constructs from donor 2 exhibited significantly decreased instantaneous modulus and Young's modulus by 0.6-fold and 0.3-fold, respectively, compared to treated P5 constructs, while there were no significant differences in the compressive relaxation modulus and UTS between the treated P5 and P9 constructs. Coefficient of viscosity, toughness, resilience, and strain at failure were not significantly different between the treated P5 and P9 constructs (supplemental figure 1). Treated donor 3 neocartilages showed comparable compressive and tensile properties as a function of passage number. Coefficient of viscosity of the treated P7 and P9 constructs were comparable with or significantly improved than that of the treated P3 constructs. Toughness, resilience, and strain to failure were not significantly different among the TCL-treated human neocartilage (supplemental figure 1).

4. Discussion

The dearth of hACs and chondrocyte dedifferentiation during expansion hamper translation of tissue engineered products to human clinical use. This study sought to extend the usefulness of passaged hACs through a process involving three steps: (a) conservative chondrogenic passaging, (b) aggregate rejuvenation, and (c) tissue formation via self-assembly. An aggregate rejuvenation step was hypothesized to improve chondrogenic properties of extensively passaged hACs (i.e. low passages: P3 and P5; high passages: P7, P9, and P11). In contrast to untreated controls, aggregate rejuvenation allowed: (a) hACs at both low and high passages (i.e. P3, P5, and P7) to self-assemble into flat discs; (b) significant GAG increases at each passage; and (c) increased

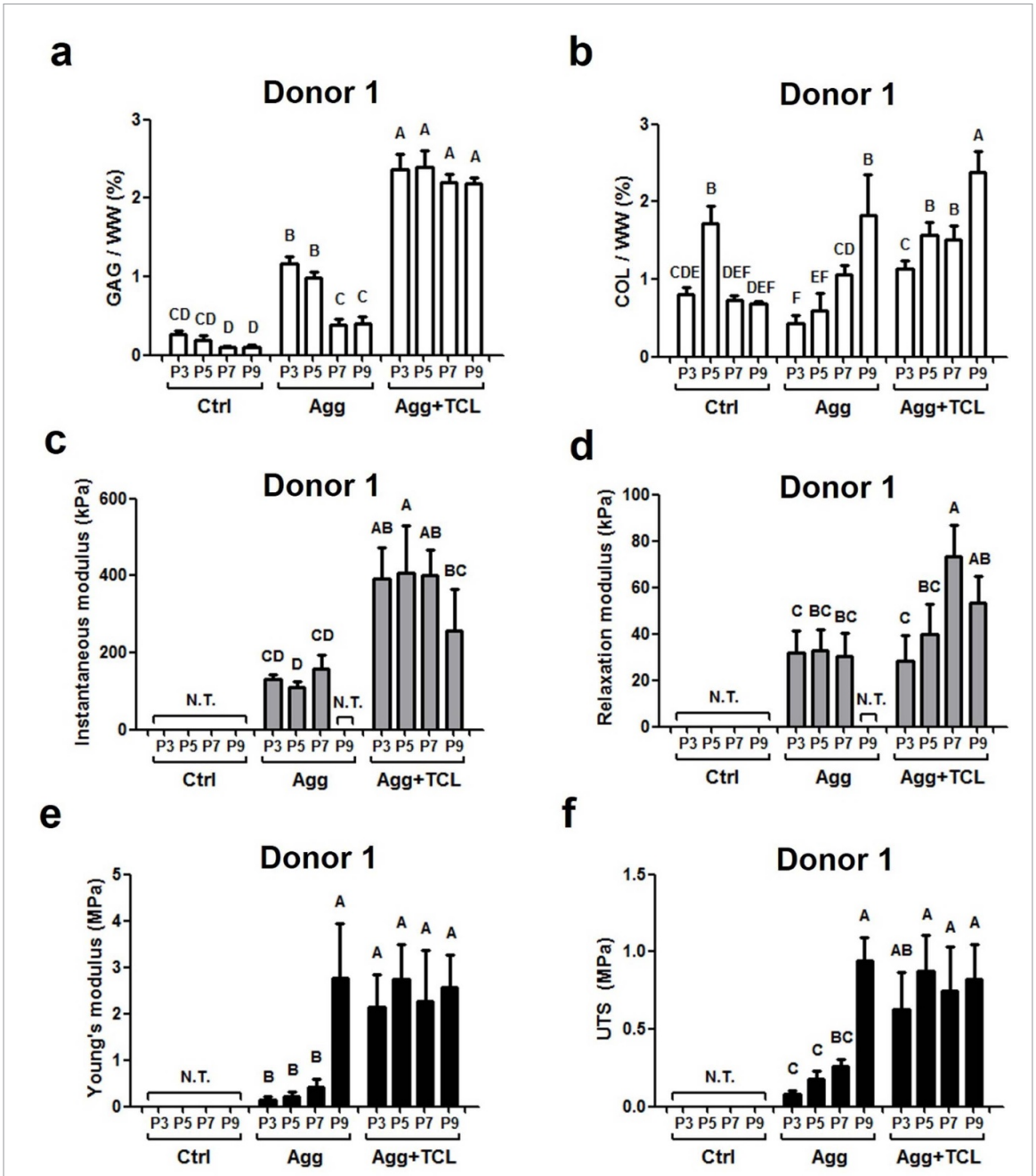

Figure 6. Biochemical and mechanical properties of human neocartilage derived from donor 1. (a) GAG content normalized by WW, (b) COL/WW, (c) instantaneous modulus, (d) relaxation modulus, (e) Young's modulus, and (f) UTS of human neocartilage constructs derived from P3, P5, P7, and P9 cells. The effects of no treatment (Ctrl), aggregate rejuvenation (Agg), and aggregate rejuvenation followed by TCL treatment (Agg + TCL) on human neocartilage are shown.

collagen content with passage number. It was also hypothesized that aggregate rejuvenation followed by TCL treatment would retain the chondrogenic potential of high passage hACs at levels of those derived from low passage hACs. When compared to constructs treated with aggregate rejuvenation only, (a) TCL treatment generated human neocartilage constructs of greater opacity and flatness at all passages; (b) with TCL treatment, both biochemical and mechanical properties of constructs derived from P7 and P9 hACs were on par with or greater than those derived from P3 and P5 hACs. Repeatability of these findings was demonstrated using two additional donors where passaging was extended to P11. This new strategy of using conservative chondrogenic passaging followed by aggregate rejuvenation on extensively passaged hACs appears to resolve the well-established limitations in human chondrocyte availability. The strategy followed by self-assembly using TCL treatment advances the use of extensively passaged hACs in cartilage repair and regeneration.

Effects of aggregate rejuvenation on construct morphology and cell phenotype were dramatic throughout all passages. Previously, morphological changes due to aggregate redifferentiation (i.e.

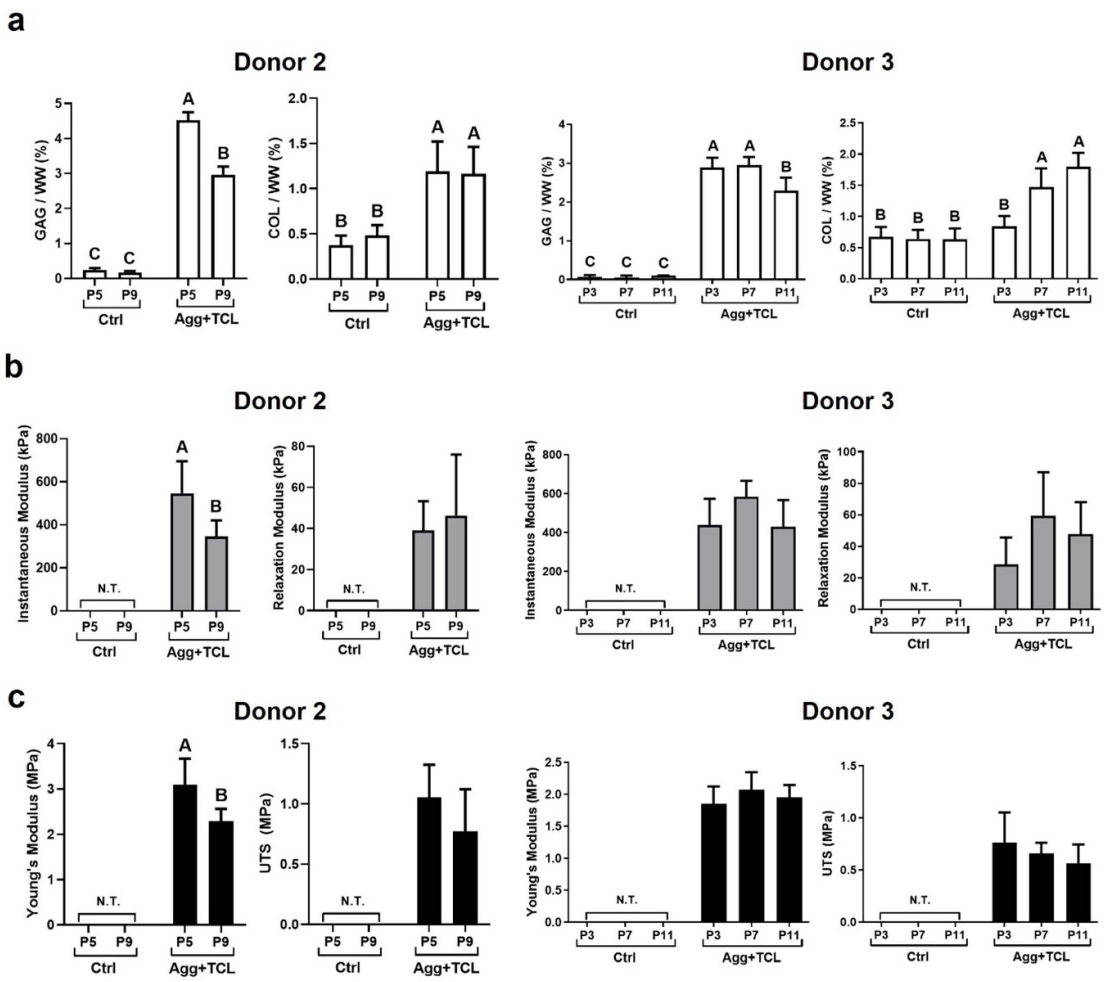

Figure 7. Biochemical and mechanical properties of human neocartilage derived from donors 2 and 3. (a) GAG and COL/WW, (b) instantaneous modulus and relaxation modulus, and (c) Young's modulus and UTS of neocartilage constructs derived from P5 and P9 donor 2 hACs, and from P3, P7, and P11 donor 3 hACs. The effects of no treatment (Ctrl), aggregate rejuvenation (Agg), and aggregate rejuvenation followed by TCL treatment (Agg + TCL) on human neocartilage are shown.

aggregate culture with TGF-β1) were seen for leporine neocartilage [18], and, similarly, aggregate rejuvenation (i.e. aggregate culture with TGF-β1, GDF-5, and BMP-2) resulted in significant changes in construct morphology of human neocartilage. Treated human cartilage retained flattened morphology up to P7 while untreated human neocartilages were curled and oblong (P3-5), or spherical (P7-9). Chondrocyte dedifferentiation is characterized by decreases in type II collagen and proteoglycan production and by an elongated fibroblastic morphology [6, 8]. By reverting dedifferentiated chondrocytes to a spherical morphology (e.g., via hydrogels [13, 14, 36] or actin cytoskeleton disruption [37, 38]), cells re-expressed a chondrogenic phenotype. In this study, untreated constructs contained hACs with fibroblastic morphology and lack of type II collagen staining. With aggregate rejuvenation treatment, hACs became rounded, embedded in lacunae, and stained for type II collagen up to P7. With increasing passage, the efficiency of aggregate rejuvenation decreased; P9 showed no type II collagen (figure 3). Nonetheless, P9 constructs treated with aggregate rejuvenation resembled untreated P3 and P5 controls, hinting at a possible 'rejuvenation' of high passage chondrocytes toward characteristics of chondrocytes of low passage numbers.

Several differences exist in the effect of aggregate culture on animal and human cells. While no major difference was found in leporine cells' production of type I and II collagen by passage number [18], a passage-dependent decrease in type II collagen and a passage-specific increase in type I collagen were found for hACs. Also, aggregate culture enhanced hACs' GAG production for all passages, but it did not influence GAG production of leporine cells [18]. Because the prior work applied only TGF-β1 on leporine cells, while this study used a combination of TGF-β1, GDF-5, and BMP-2 (TGB), the growth factors involved during aggregate culture can be another determining factor affecting matrix production at different passage numbers. However, previous studies suggest that the discrepancy may be due to species-variations, e.g., growth factor responsiveness by species. For example, in contrast to the leporine neocartilage, aggregate redifferentiation (i.e. aggregate culture with

TGF-β1) significantly increased aggrecan and collage II expression in human neocartilage [17]. In general, the effectiveness of treatments on animals or animal cells does not necessarily translate to the same results in humans or human cells. This is an exceedingly well-known fact; for example, the Food and Drug Administration states that only 8% of medical compounds that work in animals will eventually work in humans [39]. Thus, it was crucial to establish the translatability of aggregate culture of human cells toward eventual medical products for human use. Indeed, the efficacy of aggregate rejuvenation, applied after conservative chondrogenic passaging, was demonstrated in extensively passaged human cells.

This study showed that treating neocartilage with TCL following aggregate rejuvenation improved the chondrogenic phenotype of hACs at high passage numbers. As discussed above, a spherical cell shape is strongly associated with the chondrogenic phenotype [13, 14, 36–38]. While aggregate rejuvenation by itself was insufficient in rescuing P9 hACs from a fibroblastic morphology, the added TCL treatment altered P9 hACs into spherical cells in lacunae; this effect persisted up to P11. Correspondingly, type II collagen staining and GAG production were observed in TCL-treated P9 and P11 constructs. It has been well-characterized that self-assembled neocartilage derived from primary chondrocytes forms flat constructs [40, 41]. The flatter morphology of constructs derived from high passages with TCL treatment likely resulted from the morphological changes of cells to a rounded shape that is characteristic of the phenotype seen for primary chondrocytes. This correlation between cell morphology and construct morphology was also seen in P3, P5, and P7 constructs with aggregate rejuvenation (figure 2). It was also noted that high passage (P7, P9, and P11) constructs appeared smaller than those formed by cells of low passages (P3 and P5). The cause of these smaller constructs from high passages is not evident, but, for future studies, it would be beneficial to identify methods that would allow for high passage constructs to attain the same size as constructs of lower passages. These data suggest that both aggregate rejuvenation and TCL treatments promote redifferentiation of hACs, leading to chondrogenic cells capable of forming flat and robust constructs similar to those derived from primary chondrocytes.

In this study, the biochemical and, importantly, mechanical properties of high passage (P7, P9, and P11) constructs were on par with low passage (P3 and P5) constructs due to treatment with TCL. For example, with TCL treatment, GAG content increased in constructs derived from P7 and P9 hACs to a level that was not significantly different than the GAG content of TCL-treated constructs derived from P3 and P5 cells. With additional TCL treatment, the instantaneous modulus and relaxation modulus were comparable for constructs across all passage numbers. Tensile strength, toughness, resilience, and strain at failure of TCL-treated constructs were comparable across all passage numbers. Previously, neocartilage constructs derived from passaged hACs (P2), expanded and rejuvenated in the same way as the current study, but without TCL treatment, exhibited an average compressive instantaneous modulus and Young's modulus of 82 kPa and 660 kPa, respectively [16]. Excitingly, in the present study, with the addition of TCL treatment, the compressive and tensile properties exhibited up to 584 kPa (P7 constructs from donor 3) and 3 MPa (P5 constructs from donor 2). Thus, this study indicates that TCL treatment in conjunction with rejuvenation of highly passaged cells leads to enhancements in not only biochemical but also mechanical properties.

The ways by which TCL treatment alters neocartilage matrices to yield mechanically robust human neocartilage can be understood through the effects of its various parts, TGF-β1, c-ABC, and LOXL2. While TGF-β1 plays a biochemical role in cartilage matrix production, c-ABC has been shown to exhibit a biophysical role by increasing collagen fibril diameter and density [28]. LOXL2 has also been shown to modify matrix by forming PYR crosslinks among collagen fibers [27]. Fibrillar and planar substrates influence cell differentiation differently, possibly due to altered cell attachment (i.e. arrangement of focal contacts) [42], which leads to changes in cell shape, an important factor that modulates cell fate and differentiation. Cell shape, as controlled by cell attachment, has been shown to determine how mesenchymal stem cells differentiate into osteoblasts versus adipocytes [43]. The effect of cell shape has also been seen in chondrocytes: the rounded shape of chondrocytes, restored using an inhibitor of actin assembly (i.e. inhibition of cell spreading), stimulated proteoglycan synthesis [37]. These previous studies strongly indicate the significant role of interactions between cell and microenvironment in regulating cell fate and differentiation. From a tissue engineering point of view, the resulting interactions between cell and matrix can influence the functional properties of engineered neotissues. For this study, it is possible that TCL modifies cell-matrix interactions which may have yielded enhanced functional properties of constructs derived from high passages, comparable with those derived from low passages.

Monolayer expansion up to P11 and the resulting neocartilage's mechanically robust functional properties due to aggregate rejuvenation and TCL treatment can be impactful on the advancement of current therapies. It has been reported that cell yield from human articular cartilage of the medial femoral condyle was $\sim$10 000 cells mm^{-1} [44]. Thus, with

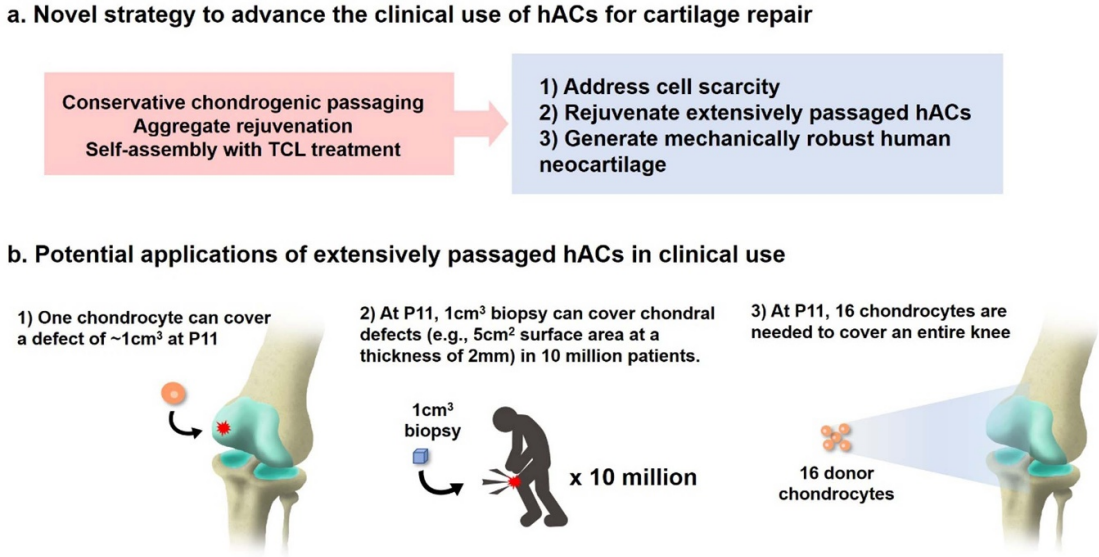

Figure 8. Novel strategy to use extensively passaged hACs for cartilage repair. (a) Conservative chondrogenic passaging, aggregate rejuvenation, and self-assembly with TCL treatment: (1) address cell scarcity, (2) rejuvenate extensively passaged hACs, and (3) generate mechanically robust human neocartilage. (b) A small number of primary hACs or a miniscule amount of cartilage will be needed to generate extensively passaged hACs (up to P11) to repair cartilage defects in the knee.

one single chondrocyte and an expansion factor of 12.6×10^6 (supplemental table 1), a 1 cm^3 neocartilage can be engineered (figure 8). Also, at P11, a 1 cm^3 cartilage biopsy can yield chondrocytes to treat defects of 5 cm^2 at a thickness of 2 mm in 10 million patients. The articular surface of an adult human knee is ~10 200 mm^2 [45]. If the thickness of articular cartilage were uniformly 2 mm, the volume of the entire knee would be ~20 400 mm^3. Thus, at P11, only 16 donor chondrocytes will be potentially needed to cover an entire knee. For knees that are larger or have thicker cartilage, more cells would be needed; the self-assembly approach has been used to engineer constructs of various sizes and thicknesses [18, 46]. Cell yield after aggregate rejuvenation, however, was significantly decreased with increasing passage number, and the level of the decrease was varied by donor (supplemental table 2). As passage number increased, the number of cells with histological appearance of a chondrogenic phenotype decreased. It is possible that aggregate rejuvenation did not convert all cells but, instead, purified the cell population by removing cells that did not possess chondrogenic potential. Further studies are needed to continue to refine these methods to improve cell yield. Nonetheless, the findings presented here provide a good starting point for resolving issues that arise from a limited availability of healthy donor cartilage.

The robustness of this study's stimuli needs to be established in future work as a function of donor age. This is because the response to TGF-β1, bFGF, and PDGF (TFP), a cocktail of growth factors used in conservative chondrogenic passaging in this study, has previously been shown to be age-dependent, and cells passaged with or without TFP may have different sensitivities to downstream processing steps, such as aggregate rejuvenation or TCL. For example, the post-expansion chondrogenic properties of TFP-treated pellets were better when the donor's age was younger than 40 [47]. In future work, it will be of interest to examine how the restoration of the chondrogenic potential, as demonstrated in this study, is affected by (a) the presence/absence of TFP, (b) cells from donors of different ages, and (c) cells that are extensively passaged (i.e. $\geqslant$P3).

Furthermore, changes in proliferation in response to TGF-β1 were found with different ages in hACs [48]. LOXL2 is known to be expressed abundantly in neonatal relative to adult equine cartilage [49]. Age-dependent changes in growth factor responsiveness and in endogenous growth factor levels warrant future investigations into applying aggregate rejuvenation and TCL treatment to hACs isolated from additional donors.

Evaluating cartilage healing response, as well as the maturation and integration of tissue engineered cartilage, *in vivo* using an animal model is a critical step toward establishing the translational potential of neocartilage. With regard to the cartilage healing response, although the functional properties of human neocartilage generated in this study are still lower than those observed in native cartilage, based on prior work, the neocartilage can still be beneficial for cartilage healing. Previously, cartilage implants, generated from porcine rib cartilage cells, exhibited, on average, only 42% of the biochemical and biomechanical properties of the native tissue, but these implants demonstrated outstanding healing and signs of remodeling after 8 weeks in temporomandibular

joint defects in minipigs [50]. This prior study suggests that implants intended for cartilage repair do not need to be identical to native cartilage to achieve healing. Thus, although our engineered human neocartilages' biochemical and mechanical properties are lower than those of native cartilage, there is potential for the human neocartilages created as described here to mature *in vivo* and to elicit a healing response in a cartilage defect. With regard to maturation *in vivo*, a previous study has shown that pre-treatment of LOXL2 *in vitro* significantly promoted maturation of neocartilage in an *in vivo* model with enhanced tensile properties and PYR content by 3 and 14-fold, respectively [27]. Finally, in terms of integration, LOXL2-treated engineered constructs were shown to integrate with native articular cartilage *in vitro* with ∼2 times greater interfacial tensile strength than control constructs [51]. Further, it has been shown that priming neofibrocartilage with TCL treatment led to enhanced integration with native fibrocartilage *in vivo*; both interfacial tensile stiffness and strength increased by ∼7-fold [29]. These previous reports suggest that *in vitro* stimuli can act as 'pre-treatments' that carry over *in vivo* to enhance implant maturation and integration. In the future, whether TCL can serve as a pre-treatment for human neocartilage implants needs to be investigated. Additionally, evaluation of any potential loss of function of regenerated neocartilage in the *in vivo* environment should also be assessed (e.g. dedifferentiation and hypertrophy). Subsequent investigations on the maturation of TCL-treated human neocartilage with respect to passage number, as well as the effect of the pre-treatment responsible for integration with native tissue in an *in vivo* model, will be necessary to further promote the treatment of aggregate rejuvenation and TCL for clinical uses.

5. Conclusion

Inherently limited access to sufficient numbers of primary hACs necessitates cell expansion. The present study identified an effective strategy to address the perennial problems of chondrocyte scarcity and rapid dedifferentiation, using conservative chondrogenic passaging and aggregate rejuvenation to achieve successful redifferentiation of cells at an expansion factor of 12.6×10^6 and a cell doubling number of ∼24. It also allowed the tissue engineering of functional human neocartilage from extensively passaged hACs up to P11, using the self-assembling process in conjunction with TCL treatment. Without aggregate rejuvenation, the chondrogenic phenotype was lost. Aggregate rejuvenation by itself elicited significant changes in construct and cell morphologies, resulting in flattened constructs with chondrogenic phenotype present, formed from cells passaged up to P7. The addition of TCL treatment following aggregate rejuvenation generated constructs with flat construct morphology and cells in lacunae for all passage numbers including P9 and P11. Even at high passages, a combination of aggregate rejuvenation and TCL treatment yielded neocartilage with functional properties on par with or greater than those of neocartilage derived from low passages. These results show that the challenge of using hACs at high passages may be overcome. This study's well-defined protocol for recovering the utility of extensively expanded hACs may be useful in advancing the translational use of tissue-engineered products for cartilage repair and regeneration.

Acknowledgments

The authors acknowledge funding support by the National Institutes of Health (NIH), R01AR067821.

ORCID iD

Kyriacos A Athanasiou https://orcid.org/0000-0001-5387-8405

References

[1] Steadman J R, Rodkey W G and Rodrigo J J 2001 Microfracture: surgical technique and rehabilitation to treat chondral defects *Clin. Orthop. Relat. Res.* **391** S362–9
[2] Hangody L, Rathonyi G K, Duska Z, Vasarhelyi G, Fules P and Modis L 2004 Autologous osteochondral mosaicplasty: surgical technique *J. Bone Joint Surg. Am.* **86-A** 65–72
[3] Dunkin B S and Lattermann C 2013 New and emerging techniques in cartilage repair: MACI *Oper. Tech. Sports Med.* **21** 100–7
[4] Kwon H, Brown W E, Lee C A, Wang D, Paschos N, Hu J C and Athanasiou K A 2019 Surgical and tissue engineering strategies for articular cartilage and meniscus repair *Nat. Rev. Rheumatol.* **15** 550–70
[5] Huang B J, Hu J C and Athanasiou K A 2016 Cell-based tissue engineering strategies used in the clinical repair of articular cartilage *Biomaterials* **98** 1–22
[6] Lin Z, Fitzgerald J B, Xu J, Willers C, Wood D, Grodzinsky A J and Zheng M H 2008 Gene expression profiles of human chondrocytes during passaged monolayer cultivation *J. Orthop. Res.* **26** 1230–7
[7] Darling E M and Athanasiou K A 2005 Rapid phenotypic changes in passaged articular chondrocyte subpopulations *J. Orthop. Res.* **23** 425–32
[8] Schulze-Tanzil G 2009 Activation and dedifferentiation of chondrocytes: implications in cartilage injury and repair *Ann. Anat.* **191** 325–38
[9] Schulze-Tanzil G, de Souza P, Villegas Castrejon H, John T, Merker H J, Scheid A and Shakibaei M 2002 Redifferentiation of dedifferentiated human chondrocytes in high-density cultures *Cell Tissue Res.* **308** 371–9
[10] Kang S W, Yoo S P and Kim B S 2007 Effect of chondrocyte passage number on histological aspects of tissue-engineered cartilage *Biomed. Mater. Eng.* **17** 269–76
[11] Jakob M, Demarteau O, Schafer D, Hintermann B, Dick W, Heberer M and Martin I 2001 Specific growth factors during the expansion and redifferentiation of adult human articular chondrocytes enhance chondrogenesis and cartilaginous tissue formation *in vitro J. Cell. Biochem.* **81** 368–77

[12] Barbero A, Ploegert S, Heberer M and Martin I 2003 Plasticity of clonal populations of dedifferentiated adult human articular chondrocytes *Arthritis Rheum.* **48** 1315–25
[13] Benya P D and Shaffer J D 1982 Dedifferentiated chondrocytes reexpress the differentiated collagen phenotype when cultured in agarose gels *Cell* **30** 215–24
[14] Caron M M, Emans P J, Coolsen M M, Voss L, Surtel D A, Cremers A, van Rhijn L W and Welting T J M 2012 Redifferentiation of dedifferentiated human articular chondrocytes: comparison of 2D and 3D cultures *Osteoarthr. Cartil.* **20** 1170–8
[15] Wolf F, Candrian C, Wendt D, Farhadi J, Heberer M, Martin I and Barbero A 2008 Cartilage tissue engineering using pre-aggregated human articular chondrocytes *Eur. Cells Mater.* **16** 92–9
[16] Huey D J and Athanasiou K A 2013 Alteration of the fibrocartilaginous nature of scaffoldless constructs formed from leporine meniscus cells and chondrocytes through manipulation of culture and processing conditions *Cells Tissues Organs* **197** 360–71
[17] Murphy M K, Huey D J, Hu J C and Athanasiou K A 2015 TGF-beta1, GDF-5, and BMP-2 stimulation induces chondrogenesis in expanded human articular chondrocytes and marrow-derived stromal cells *Stem. Cells* **33** 762–73
[18] Huang B J, Hu J C and Athanasiou K A 2016 Effects of passage number and post-expansion aggregate culture on tissue engineered, self-assembled neocartilage *Acta Biomater.* **43** 150–9
[19] Kwon H, Paschos N K, Hu J C and Athanasiou K 2016 Articular cartilage tissue engineering: the role of signaling molecules *Cell. Mol. Life Sci.* **73** 1173–94
[20] Blunk T, Sieminski A L, Gooch K J, Courter D L, Hollander A P, Nahir A M, Langer R, Vunjak-Novakovic G and Freed L E 2002 Differential effects of growth factors on tissue-engineered cartilage *Tissue Eng.* **8** 73–84
[21] Elder B D and Athanasiou K A 2009 Systematic assessment of growth factor treatment on biochemical and biomechanical properties of engineered articular cartilage constructs *Osteoarthr. Cartil.* **17** 114–23
[22] Bian L, Crivello K M, Ng K W, Xu D, Williams D Y, Ateshian G A and Hung C T 2009 Influence of temporary chondroitinase ABC-induced glycosaminoglycan suppression on maturation of tissue-engineered cartilage *Tissue Eng.* A **15** 2065–72
[23] Natoli R M, Revell C M and Athanasiou K A 2009 Chondroitinase ABC treatment results in greater tensile properties of self-assembled tissue-engineered articular cartilage *Tissue Eng.* A **15** 3119–28
[24] Natoli R M, Responte D J, Lu B Y and Athanasiou K A 2009 Effects of multiple chondroitinase ABC applications on tissue engineered articular cartilage *J. Orthop. Res.* **27** 949–56
[25] Eyre D 1987 Collagen cross-linking amino acids *Meth. Enzymol.* **144** 115–39
[26] Siegel R C 1976 Collagen cross-linking. Synthesis of collagen cross-links *in vitro* with highly purified lysyl oxidase *J. Biol. Chem.* **251** 5786–92
[27] Makris E A, Responte D J, Paschos N K, Hu J C and Athanasiou K A 2014 Developing functional musculoskeletal tissues through hypoxia and lysyl oxidase-induced collagen cross-linking *Proc. Natl Acad. Sci. USA* **111** E4832–41
[28] Responte D J, Arzi B, Natoli R M, Hu J C and Athanasiou K A 2012 Mechanisms underlying the synergistic enhancement of self-assembled neocartilage treated with chondroitinase-ABC and TGF-beta1 *Biomaterials* **33** 3187–94
[29] Makris E A, MacBarb R F, Paschos N K, Hu J C and Athanasiou K A 2014 Combined use of chondroitinase-ABC, TGF-beta1, and collagen crosslinking agent lysyl oxidase to engineer functional neotissues for fibrocartilage repair *Biomaterials* **35** 6787–96
[30] Kwon H, O'Leary S A, Hu J C and Athanasiou K A 2019 Translating the application of transforming growth factor-beta1, chondroitinase-ABC, and lysyl oxidase-like 2 for mechanically robust tissue-engineered human neocartilage *J. Tissue Eng. Regen. Med.* **13** 283–94
[31] Athanasiou K A, Eswaramoorthy R, Hadidi P and Hu J C 2013 Self-organization and the self-assembling process in tissue engineering *Annu. Rev. Biomed. Eng.* **15** 115–36
[32] Hu J C and Athanasiou K A 2006 A self-assembling process in articular cartilage tissue engineering *Tissue Eng.* **12** 969–79
[33] Huey D J, Hu J C and Athanasiou K A 2013 Chondrogenically tuned expansion enhances the cartilaginous matrix-forming capabilities of primary, adult, leporine chondrocytes *Cell Transplant.* **22** 331–40
[34] Mow V C, Kuei S C, Lai W M and Armstrong C G 1980 Biphasic creep and stress relaxation of articular cartilage in compression? Theory and experiments *J. Biomech. Eng.* **102** 73–84
[35] Cissell D D, Link J M, Hu J C, Athanasiou K A and Modified Hydroxyproline A 2017 Assay based on hydrochloric acid in Ehrlich's solution accurately measures tissue collagen content *Tissue Eng.* C **23** 243–50
[36] Bonaventure J, Kadhom N, Cohen-Solal L, Ng K H, Bourguignon J, Lasselin C and Freisinger P 1994 Reexpression of cartilage-specific genes by dedifferentiated human articular chondrocytes cultured in alginate beads *Exp. Cell Res.* **212** 97–104
[37] Newman P and Watt F M 1988 Influence of cytochalasin D-induced changes in cell shape on proteoglycan synthesis by cultured articular chondrocytes *Exp. Cell Res.* **178** 199–210
[38] Rottmar M, Mhanna R, Guimond-Lischer S, Vogel V, Zenobi-Wong M and Maniura-Weber K 2014 Interference with the contractile machinery of the fibroblastic chondrocyte cytoskeleton induces re-expression of the cartilage phenotype through involvement of PI3K, PKC and MAPKs *Exp. Cell Res.* **320** 175–87
[39] US Food and Drug Administration 2004 Innovation or stagnation: challenge and opportunity on the critical path to new medical products
[40] Revell C M, Reynolds C E and Athanasiou K A 2008 Effects of initial cell seeding in self assembly of articular cartilage *Ann. Biomed. Eng.* **36** 1441–8
[41] Ofek G, Revell C M, Hu J C, Allison D D, Grande-Allen K J and Athanasiou K A 2008 Matrix development in self-assembly of articular cartilage *PLoS One* **3** e2795
[42] Reilly G C and Engler A J 2010 Intrinsic extracellular matrix properties regulate stem cell differentiation *J. Biomech.* **43** 55–62
[43] McBeath R, Pirone D M, Nelson C M, Bhadriraju K and Chen C S 2004 Cell shape, cytoskeletal tension, and RhoA regulate stem cell lineage commitment *Dev. Cell* **6** 483–95
[44] Hunziker E B, Quinn T M and Hauselmann H J 2002 Quantitative structural organization of normal adult human articular cartilage *Osteoarthr. Cartil.* **10** 564–72
[45] Hohe J, Ateshian G, Reiser M, Englmeier K H and Eckstein F 2002 Surface size, curvature analysis, and assessment of knee joint incongruity with MRI *in vivo Magn. Reson. Med.* **47** 554–61
[46] Huang B J, Brown W E, Keown T, Hu J C and Athanasiou K A 2018 Overcoming challenges in engineering large, scaffold-free neocartilage with functional properties *Tissue Eng.* A **24** 1652–62
[47] Barbero A, Grogan S, Schafer D, Heberer M, Mainil-Varlet P and Martin I 2004 Age related changes in human articular chondrocyte yield, proliferation and post-expansion chondrogenic capacity *Osteoarthr. Cartil.* **12** 476–84
[48] Guerne P A, Blanco F, Kaelin A, Desgeorges A and Lotz M 1995 Growth factor responsiveness of human articular chondrocytes in aging and development *Arthritis Rheum.* **38** 960–8
[49] Mienaltowski M J, Huang L, Stromberg A J and MacLeod J N 2008 Differential gene expression associated with postnatal

equine articular cartilage maturation *BMC Musculoskelet. Disord.* **9** 149

[50] Vapniarsky N, Huwe L W, Arzi B, Houghton M K, Wong M E, Wilson J W, Hatcher D C, Hu J C and Athanasiou K A 2018 Tissue engineering toward temporomandibular joint disc regeneration *Sci. Transl. Med.* **10** 446

[51] Athens A A, Makris E A and Hu J C 2013 Induced collagen cross-links enhance cartilage integration *PLoS One* **8** e60719